Taylor & Francis
Taylor & Francis Group

ORIGINAL RESEARCH

🔓 OPEN ACCESS   ✓ Check for updates

A Virus-Like-Particle immunotherapy targeting Epitope-Specific anti-xCT expressed on cancer stem cell inhibits the progression of metastatic cancer *in vivo*

Elisabetta Bolli[a], John P. O'Rourke [iD][b], Laura Conti[a], Stefania Lanzardo[a], Valeria Rolih[a], Jayne M. Christen[b], Giuseppina Barutello[a], Marco Forni[c], Federica Pericle[b,#], and Federica Cavallo [iD][a,#]

[a]Department of Molecular Biotechnology and Health Sciences, Molecular Biotechnology Center, University of Torino, Torino, Italy; [b]Agilvax, Inc, Albuquerque, NM, United States of America; [c]EuroClone S.p.A Research Laboratory, Molecular Biotechnology Center, University of Torino, Torino, Italy

ABSTRACT

Aggressive forms of breast cancer, such as Her2+ and triple negative breast cancer (TNBC), are enriched in breast cancer stem cells (BCSC) and have limited therapeutic options. BCSC represent a key cellular reservoir for relapse, metastatic progression and therapeutic resistance. Their ability to resist common cytotoxic therapies relies on different mechanisms, including improved detoxification. The cystine-glutamate antiporter protein xCT (SLC7A11) regulates cystine intake, conversion to cysteine and subsequent glutathione synthesis, protecting cells against oxidative and chemical insults. Our previous work showed that xCT is highly expressed in tumorspheres derived from breast cancer cell lines and downregulation of xCT altered BCSC function *in vitro* and inhibited pulmonary metastases *in vivo*. We further strengthened these observations by developing a virus-like-particle (VLP; AX09-0M6) immunotherapy targeting the xCT protein. AX09-0M6 elicited a strong antibody response against xCT including high levels of IgG2a antibody. IgG isolated from AX09-0M6 treated mice bound to tumorspheres, inhibited xCT function as assessed by reactive oxygen species generation and decreased BCSC growth and self-renewal. To assess if AX09-0M6 impacts BCSC *in vivo* seeding, Her2+ TUBO-derived tumorspheres were injected into the tail vein of AX09-0M6 or control treated female BALB/c mice. AX09-0M6 significantly inhibited formation of pulmonary nodules. To evaluate its ability to impact metastases, AX09-0M6 was administered to mice with established subcutaneous 4T1 tumors. AX09-0M6 administration significantly hampered tumor growth and development of pulmonary metastases. These data show that a VLP-based immunization approach inhibits xCT activity, impacts BCSC biology and significantly reduces metastatic progression in preclinical models.

Introduction

It is estimated that in 2017, 252,000 women will be diagnosed with breast cancer in the United States including 30,000 new cases of triple negative breast cancer (TNBC), a highly aggressive form of breast cancer.[1] According to the hierarchical cancer model, mammary tumors, as the majority of cancers, are organized in a cellular hierarchy with cancer stem cells (CSC) at the apex.[2] CSC are often enriched in highly metastatic breast cancers, including TNBC and Her2+ breast cancer.[3] CSC have the unique biological properties necessary for maintenance and spreading of the tumor, and through asymmetric division can differentiate into cancer cells that compose the tumor bulk.[4,5] Due to their resistance to traditional radiation and chemotherapies,[6] CSC represent a reservoir for the relapse, metastatic evolution and progression of the disease after treatment. Therefore, successful eradication of CSC represents a major barrier towards effective cancer treatments.

The ability of CSC to resist common cytotoxic therapies relies on different mechanisms, including improved detoxification ability. The cystine-glutamate antiporter protein xCT (SLC7A11), the light chain of the antiporter system x_c^-, regulates cystine intake, conversion to cysteine and subsequent glutathione (GSH) synthesis, protecting cells against oxidative and chemical insults.[7,8] xCT is a 12 multi-pass transmembrane protein, characterized by 6 extracellular domains (named ECD1-6), in which the N- and C-termini are located intracellularly.[9] xCT expression is low in normal cells and highly restricted to a few cell types (astrocytes, microglia and other subsets of myeloid cells),[10,11] but elevated levels of xCT protein are observed in a high percentage of mammary tumors including TNBC.[12] High levels of xCT mRNA and protein correlate with significant reduction in distal metastases-free and overall survival.[13,14] xCT expression is upregulated in breast CSC (BCSC)[15] and other solid tumor stem cells,[16–21] and several studies show that xCT physically interacts with the

well-known stem cell proteins, CD44 and MUC1.[6,20–23] The frequency of xCT expression on a variety of CSC suggests that therapies targeting xCT may be effective in treating many tumors with high stem cell frequencies including gastrointestinal[23] and pancreatic[24] cancers.

Our published work established xCT as an immunotherapeutic target for BCSC.[12] Microarray analysis identified xCT as a gene that was upregulated in BCSC and subsequent studies confirmed xCT upregulation in human and murine BCSC.[12] Inhibition of xCT function resulted in a significant decrease of BCSC viability, reduced self-renewal and altered cellular redox levels.

A direct role for xCT in breast cancer growth and metastasis was shown by immunizing mice with a DNA-based vaccine expressing the full-length xCT protein.[12] Administration of the xCT vaccine prior to or in mice with existing tumors resulted in significantly decreased pulmonary metastases and tumors containing significantly less BCSC compared to control animals. The combination of xCT vaccination and chemotherapy synergistically reduced metastatic disease compared to mice that were treated with either therapy alone.[12] Similar results were observed by inhibiting xCT function with the small molecule sulfasalazine (SASP),[6,7,25,26] a Food and Drug Administration (FDA)-approved anti-inflammatory drug characterized by low specificity for xCT, short bioavailability and numerous side effects.[27,28]

The mechanism of action for DNA vaccination usually acts through cytotoxic CD8 T cell activation. However, there was no T-cell response to the major xCT T-cell epitope in DNA vaccinated mice, and immunization in B-cell deficient mice showed inadequate therapeutic responses.[12] IgG antibodies isolated from the sera of vaccinated mice inhibited BCSC function *in vitro* in a similar manner as siRNA and SASP treatment, demonstrating that vaccine-induced xCT antibodies represented the therapeutic effectors.[12] However, antibody titers achieved using the DNA vaccine were low, suggesting that the development of new therapies generating a focused, high titer antibody response would lead to greater inhibition of metastatic progression.

Virus-like particle (VLP) vaccines generate strong immune responses[29] due to their optimal size, particulate nature, and potent intrinsic adjuvant activity.[30] Agilvax's VLP technology is derived from a family of single-stranded RNA bacteriophages, including MS2, PP7, Qß, and AP205. To create a VLP that was more thermodynamically stable and dramatically more tolerant of foreign AB loop peptide insertions, Agilvax engineered a single-chain dimer version of the MS2 coat protein. Resulting VLPs are comprised of a single coat protein that self-assembles into a 27 nm diameter icosahedral particle consisting of 90 coat protein dimers. Our VLP technology allows for the precise control of epitope size, structure (loop/linear) and valency to optimize immune responses for a specific antigen.[31–34] Epitopes are displayed in an ordered, geometric pattern on the surface of the VLPs and elicit robust antibody responses, even against self-antigens.[35–37] In this paper, we produced and tested a novel VLP-based immunotherapy (AX09-0M6) that displays the 6th extracellular domain (ECD6) of human xCT in the AB surface loop on the MS2 VLP. Dosing of BALB/c mice with AX09-0M6 generated high titer antibodies that bound to xCT expressing BCSC and these antibodies inhibited BCSC function *in vitro*. Mice immunized with AX09-0M6 had significantly less

pulmonary metastases compared to controls in syngeneic models of breast cancer.

Results

Construction of xCT VLPs

To construct a VLP-based immunotherapy targeting xCT, we identified five (out of six) potential ECD from the human xCT structure to display on the surface of our VLP technology (Fig. 1A). The various ECD of human xCT were cloned into the coat protein (CP) AB loop rather than in a linear display point of our VLP to more closely mimic the native cellular structure of the xCT domains. The VLPs were expressed in *E. coli*, purified (Fig. 1B) and initial characterization showed that VLPs displaying ECD1, ECD3 and ECD6 assembled properly. Based upon ECD6 full homology in human and mouse xCT sequence, the VLP displaying the ECD6 peptide (AX09-0M6) was used for the pre-clinical studies reported here.

AX09-0M6 administration induces a functional xCT antibody response

To evaluate antibody responses, female BALB/c mice were immunized two times in the absence of exogenous adjuvant
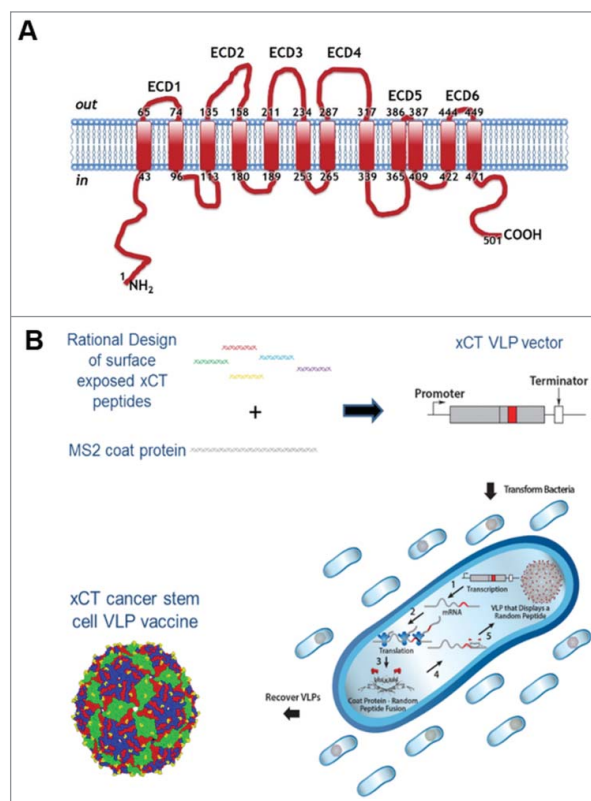
Figure 1. xCT structure and VLP production. (A) Human xCT contains six extracellular domains that range from 2 aa (ECD5) to 31 aa (ECD4) (NCBI Reference Sequence: NP_055146.1). The human ECDs exhibit high homology to mouse with ECD6 showing 100% identity. (B) Production of xCT VLPs. The single chain MS2 coat protein (CP) was synthesized to contain an individual xCT ECD displayed in the AB loop domain to more closely mimic native xCT structure. Plasmids were introduced into cells by transformation where MS2 CP self assembles into VLPs. Bacteria were lysed and VLPs were purified from the soluble protein fraction. The xCT VLPs differ from wild-type MS2 VLPs only in the xCT ECD peptide displayed in the surface exposed AB loop.

with AX09-0M6 or control MS2 wild-type (MS2 wt) and a peptide ELISA was used to measure the end-point titer. Sera from AX09-0M6 treated BALB/c mice were serially diluted and incubated with xCT ECD6 peptide coated wells and specific antibody binding was analyzed by ELISA. AX09-0M6 generated peptide antibody titers from 5×10^2 to 1.4×10^4 with an average of 3×10^3 (Fig. 2A), whereas no detectable binding was observed in mice treated with MS2 wt. Immune sera were also analyzed for relative amounts of different IgG isotypes. AX09-0M6 induced high levels of IgG2a compared to IgG1, indicative of a Th1 biased antibody response (Fig. 2B). IgG2b levels were also elevated compared to IgG1 (Fig. 2B), while little detectable IgG3 was observed (data not shown).

To analyze the ability of AX09-0M6 induced antibodies to bind BCSC, tumorspheres derived from TUBO (mouse HER2$^+$; Fig. 2C), 4T1 (mouse TNBC; Fig. 2D), HCC-1806 (human TNBC; Fig. 2E) and MDA-MB-231 (human TNBC; Fig. 2F) cells were incubated with IgG purified from sera of mice vaccinated with AX09-0M6 or MS2 wt and analyzed by FACS. A commercial anti-xCT Ab was used as a control. IgG from AX09-0M6 vaccinated mice bound to both mouse and human xCT$^+$ BCSC, while no signal was observed with IgG from MS2 wt treated mice.

These results were confirmed by the ability of IgG purified from AX09-0M6-immunized mouse sera to stain tumorspheres derived from TUBO (Fig. 3A), 4T1 (Fig. 3B), HCC-1806 (Fig. 3C) and MDA-MB-231 (Fig. 3D) cells, as shown by confocal images (Fig. 3, on the left) and fluorescent signal quantification graphs, calculated as integrated density normalized to nuclei number (Fig. 3, on the right). No binding was observed in cells incubated with purified IgG from MS2 wt treated mice.

Antibodies induced by AX09-0M6 inhibit BCSC function

To test the effect exerted by anti-xCT antibodies induced by VLP vaccination on BCSC, tumorspheres generated from TUBO cells were incubated for 5 days with IgG purified from the sera of vaccinated mice or with the xCT inhibitor sulfasalazine (SASP). As reported in Fig. 4A, IgG from MS2 wt treated mice did not affect BCSC, while those purified from AX09-0M6 vaccinated mice reduced the number (Fig. 4A, panel i) and dimension of spheres (Fig. 4A, panel ii and Supplementary Fig. 1A), exerting an effect comparable to SASP. This reduced sphere-generation ability was accompanied by both a decrease in the percentage of BCSC, evaluated as cells positive for the Aldefluor reagent that measures aldehyde dehydrogenase-1 activity (Fig. 4A, panel iii), and an increase in Reactive Oxygen Species (ROS) content as compared with MS2 wt (Fig. 4A, panel iv).

The ability of anti-xCT antibodies induced by VLP vaccination to inhibit BCSC was not restricted to the TUBO model, as similar results were obtained in other murine (4T1; Fig. 4B and Supplementary Figure 1B) and human (HCC-1806 and MDA-MB-231, Fig. 4C, D and Supplementary Fig. 1C, D) TNBC cell lines. These results suggest that AX09-0M6 elicits anti-xCT antibodies affecting BCSC self-renewal ability.

ROS levels are regulated by xCT via production of GSH, and inhibition of xCT function using a variety of approaches results in an increase in intracellular ROS levels.[12] To investigate if

AX09-0M6 elicits antibodies that inhibit xCT function, tumorspheres were incubated for 5 days with IgG purified from MS2 wt or AX09-0M6 vaccinated animals. As seen in Fig. 4 (panel iv), IgG from AX09-0M6 mice resulted in a significant increase in the intracellular ROS levels similar to SASP. In contrast, there were no differences in ROS levels from tumorspheres incubated with IgG from MS2 wt sera, suggesting that AX09-0M6 elicits antibodies that bind to and inhibit xCT function.

AX09-0M6 treatment has limited or no effect on normal tissues expressing xCT

Since xCT is expressed at low levels by mouse (but not human) spleen myeloid cells,[38] we analyzed the relative amount of these cell populations in the spleen of vaccinated mice as compared to untreated or MS2 wt treated mice. As shown in Fig. 5A, AX09-0M6 did not induce any reduction in dendritic cells, neutrophils, and macrophages. When xCT$^+$ cells were evaluated, no significant alterations were found (Fig. 5B), but there was a trend towards a reduction in xCT$^+$ neutrophils and macrophages (Fig. 5B). In the case of macrophages, the reduction was primarily found in the M1 and M0 subsets (Fig. 5C).

In the mouse, xCT is also expressed in the central nervous system by astrocytes and microglia.[10,11] In order to exclude brain toxicity in vaccinated mice, we performed a histological and immunohistochemical analysis of brains from AX09-0M6 vaccinated BALB/c mice whose sera endpoint titers are reported in Fig. 2A. Haematoxylin and Eosin (H&E) staining showed no significant morphological alterations and lesions, which suggests that vaccination-induced toxicity was not present. Slight lesions of uncertain meaning, artifacts or agonics, and tiny lymphocytic infiltrates have been detected, but they were distributed in all groups (untreated, MS2 wt and AX09-0M6 treated; data not shown). Immunohistochemical analysis with the F4/80 microglial marker did not reveal any alterations and differences in the AX09-0M6 treated group versus the MS2 wt treated and untreated groups (Fig. 5D-F). Similarly, no significant inflammatory cell infiltrates or any other abnormalities were detected in H&E-stained sections of brains from outbred CD-1 mice (data not shown) in which immunization with AX09-0M6 generated very robust endpoint titers (Supplementary Fig. 2A). The lack of toxicity was also supported by the absence of any detectable behavioural changes, such as increased aggressiveness, narcolepsy or uncoordinated movements, in living AX09-0M6 mice.

AX09-0M6 attenuates experimental metastases in vivo affecting the immune infiltrate

To evaluate the ability of AX09-0M6 to inhibit CSC mediated seeding and resuming growth at the metastatic site in vivo, we used a well-characterized preventive mouse cancer model.[12,39] Female BALB/c mice were vaccinated twice at two-week intervals with MS2 wt or AX09-0M6. One week after final boost, mice were injected intravenously (i.v.) with TUBO-derived tumorspheres and the number of micrometastases was evaluated histologically three weeks later. Mice treated with AX09-0M6 had a significant decrease (~42%) in the number of pulmonary metastases compared to control animals (Fig. 6A).
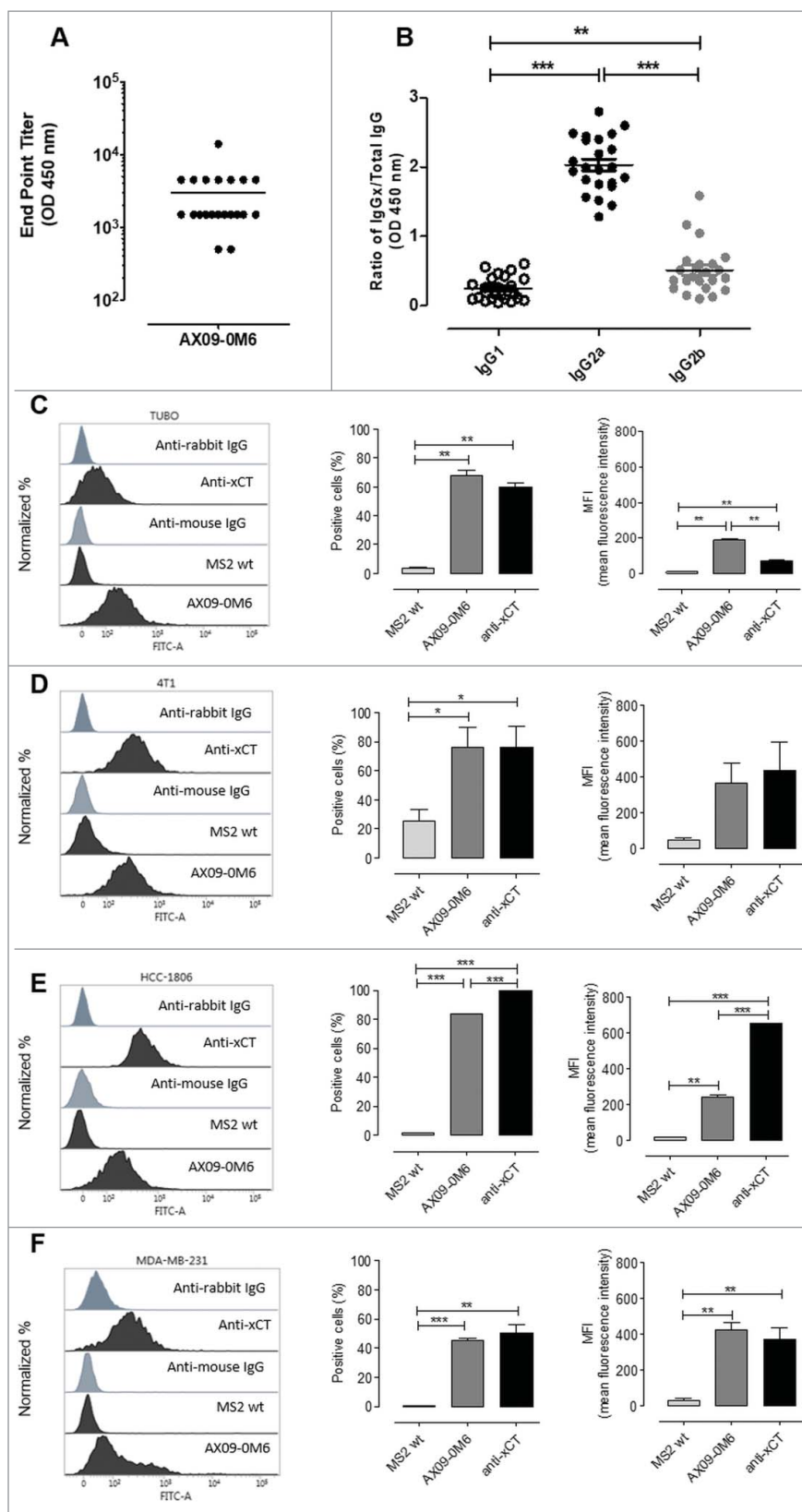
Figure 2. AX09-0M6 induced strong antibody responses. (A) Peptide ELISA of sera from treated BALB/c mice were serially diluted and incubated with xCT ECD6 peptide coated wells. End-point titers were determined by the highest dilution that was 2-fold over background. No titer was observed with control sera. Each dot represents an individual animal treated with AX09-0M6 and results are from 3 independent experiments. (B) AX09-0M6 sera from panel A were analyzed for relative amounts of different IgG isotypes. The relative ratio of each IgG subclass was calculated for each animal by taking the average OD_{450} value from a given IgG subclass (IgGx) divided by the average OD_{450} from total IgG. (C-F) FACS analysis of tumorspheres derived from TUBO (C), 4T1 (D), HCC-1806 (E) or MDA-MB-231 (F) cells incubated with 50 μg/ml IgG purified from sera of MS2 wt or AX09-0M6-vaccinated mice, or with a commercial anti-xCT Ab. Representative histograms are shown. Graphs show the mean $\pm$ SEM of the percentage of positive cells set on the base of FITC-conjugated secondary Ab staining and of mean fluorescence intensity from 3 independent experiments. *, P < 0.05; **, P < 0.01, ***, P < 0.001, Student's t-test .
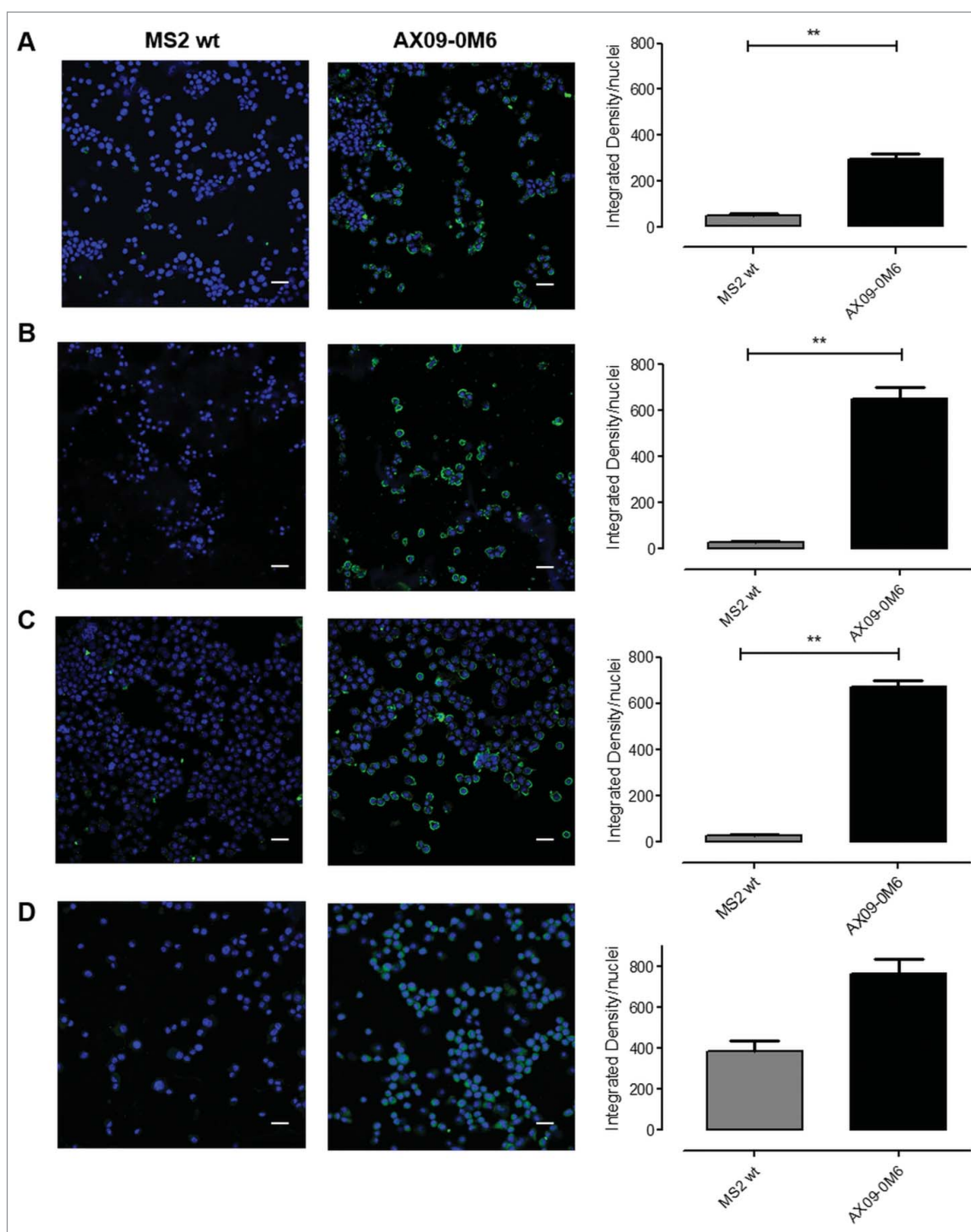
Figure 3. AX09-0M6-induced antibodies target tumorspheres. Representative immunofluorescence images of TUBO (A), 4T1 (B), HCC-1806 (C) and MDA-MB-231 (D)-derived tumorspheres incubated with IgG (50 μg/ml) purified from sera of BALB/c mice vaccinated with MS2 wt or AX09-0M6. The specific signal (green) was detected with an Alexa Fluor488-conjugated anti-mouse secondary antibody. Nuclei were counterstained with DAPI (blue). Magnification 40X, Scale bar, 40 μm [**], $P < 0.01$, Student's t-test.

To see if AX09-0M6 administration could alter the tumor microenvironment, immune infiltrates in lungs were assessed using FACS analysis. As shown in Fig. 6B, AX09-0M6 induced a significant increase in lung infiltrating NK cells and a trend showing an increase in T cells, while no difference in either $\gamma\delta$ T cells and NKT cells were observed compared to untreated or MS2 wt vaccinated mice. Of note, both MS2 wt and AX09-0M6 increased the proportion of CD8$^+$ T cells and decreased that of CD4$^+$ T cells when compared to untreated mice (Fig. 6C),

suggesting that VLPs may influence the tumor microenvironment independently of the expression of a specific peptide in the CP AB loop. Although not significant, MS2 wt and, to a greater extent, AX09-0M6, decreased the number of Ly6G$^+$Ly6C$^+$ neutrophils and increased both the Ly6G$^-$Ly6C$^+$ monocytes and F4/80$^+$ macrophages compared to untreated animals (Fig. 6D).

The increased number of NK cells in the lungs of AX09-0M6 treated mice and the fact that AX09-0M6 induces xCT
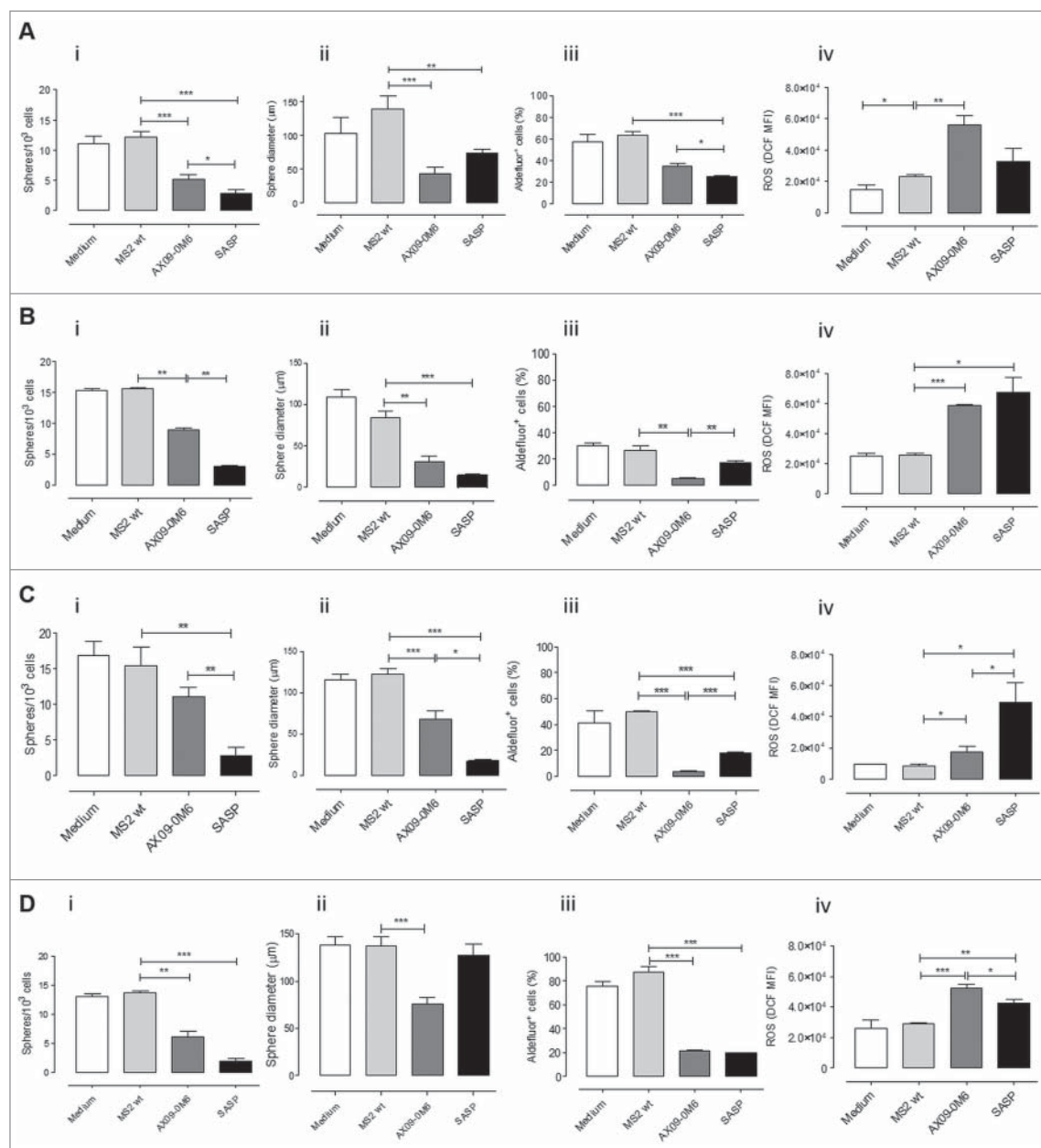
Figure 4. Vaccine-induced antibodies target CSC and affect self-renewal and ROS flux. TUBO (A), 4T1 (B), HCC-1806 (C) and MDA-MB-231 (D)-derived tumorspheres were incubated for 5 days with medium, IgG (50 μg/ml) purified from sera of BALB/c mice vaccinated with MS2 wt or AX09-0M6, or with SASP (50 μM). i) Sphere generating ability reported as tumorsphere number/10^3 plated cells. ii) Sphere diameter measured with the AxioVision 4.8 software. FACS analysis of iii) Aldefluor positivity reported as percentage of positive cells and of iv) ROS production, reported as DCF MFI. All graphs show mean $\pm$ SEM from at least three independent experiments. *, $P < 0.05$; **, $P < 0.01$, ***, $P < 0.001$, Student's t-test.

targeting antibodies mainly of the IgG2a subclass, were suggestive of a possible role of antibody-dependent cellular cytotoxicity (ADCC) in vaccine-mediated metastatic inhibition. To test this possibility, we performed an ADCC *in vitro* assay by using xCT^+ 4T1 cells as targets incubated with the sera (1:50 dilution) from mice treated with AX09-0M6, MS2 wt or left untreated and autologous splenocytes (SPC) as effectors. As shown in Fig. 6E, SPC in the presence of pooled sera from AX09-0M6 vaccinated mice mediated higher ADCC at 200:1 and 100:1 effector/target ratios than sera from MS2 wt treated ($P = 0.0595$ and $P = 0.0468$, respectively) or untreated control ($P = 0.0297$ and $P = 0.0033$, respectively) mice.

AX09-0M6 slows in vivo mammary tumor growth and attenuates spontaneous metastases

To investigate if AX09-0M6 would affect tumor growth and metastatic progression in mice with existing tumors, we used the 4T1 syngeneic therapeutic model.[40] Tumorspheres generated from 4T1 cells were administered subcutaneously (s.c.) into the mammary fat pad. When the tumors were 1 – 1.5 mm in diameter, mice were vaccinated with AX09-0M6 followed by a boost 2 weeks later. As seen in Fig. 7A, the tumor growth rate (as measured by tumor volume) was significantly slower in the AX09-0M6 treated animals compared to controls. Forty days after tumor challenge, animals were euthanized and the
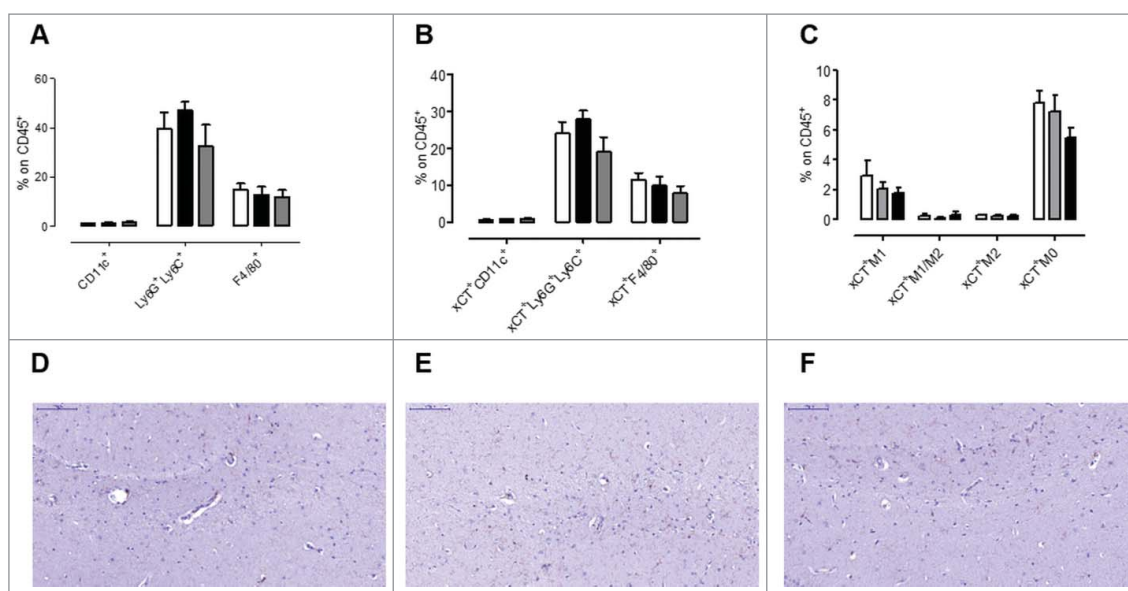
Figure 5. No signs of toxicity in the spleen and brain of AX09-0M6 treated mice. (A-C) FACS analysis of SPC from mice left untreated (white bars) or vaccinated with MS2 wt (black bars) or AX09-0M6 (gray bars). A) Percentage $\pm$ SEM of CD11c$^+$ dendritic cells, Ly6G$^+$Ly6C$^+$ neutrophils and F4/80$^+$ macrophages among the CD45$^+$ cell population. (B) Percentage $\pm$ SEM of xCT$^+$ CD11c$^+$ dendritic cells, Ly6G$^+$Ly6C$^+$ neutrophils and F4/80$^+$ macrophages among the CD45$^+$ cell population. (C) Percentage $\pm$ SEM of xCT$^+$ HLA class II$^+$ M1, HLA class II$^+$ CD206$^+$ M1/M2, CD206$^+$ M2 and HLA class II$^-$ CD206$^-$ M0 F4/80$^+$ macrophages among the CD45$^+$ cell population. (D-F) F40/80 immunohistochemical staining in brain from untreated (D), MS2 wt (E) and AX09-0M6 (F) representative mice; microglial cell processes are stained in brown. (20X, scale bar 100 μm).

number of micrometastases was measured. Similar to the preventative model, treatment with AX09-0M6 significantly inhibited the number of spontaneous pulmonary metastases compared to control animals (Fig. 7B), suggesting that AX09-0M6 might represent a new immunotherapy option for breast cancer patients.

Discussion

Our previous work showed that xCT is upregulated in human and murine BCSC and established xCT as an immunotherapeutic target for BCSC.[12] In this manuscript, we show that an active immunization approach using a VLP-based immunotherapy targeting xCT significantly decreased lung metastases in a therapeutic model of aggressive TNBC breast cancer. Moreover, this vaccination was successful in decreasing HER2$^+$ BCSC seeding, thus reducing tumor growth at the metastatic site. In the therapeutic setting, AX09-0M6 also decreased the primary tumor growth rate (as assessed by tumor volume) in the xCT positive 4T1 TNBC model,[40] suggesting that AX09-0M6 may have additional activity in the 30% of TNBC patients whose bulk tumor cells are also xCT positive.[13,26]

The mechanism of action for AX09-0M6 is mostly through the generation of an oligoclonal xCT antibody response and efficacy is therefore independent from MHC expression and can target CSC that are known to downregulate the expression of MHC class I molecules to escape cytotoxic T lymphocyte attack.[41,42] AX09-0M6 induced antibodies inhibited xCT function *in vitro* resulting in a significant decrease of BCSC viability, reduced self-renewal and altered cellular redox levels, showing

that xCT is required for BCSC function rather than simply representing a biomarker of BCSC. Therefore, AX09-0M6 treatment (and other therapies inhibiting xCT function) should not lead to cancer escape mutants via antigen loss mechanisms.[43,44]

Besides the direct effect of antibodies on xCT function, it should be noted that AX09-0M6 induced a predominant IgG2a antibody response, a subclass that has strong ADCC and Complement Dependent Cytotoxicity (CDC) activity. Indeed, sera from AX09-0M6 vaccinated mice was able to induce cytotoxicity against xCT$^+$ tumor cells. Moreover, analysis of tumor infiltrating lymphocytes (TILs) showed higher levels of NK cells in the metastatic lungs from AX09-0M6 treated animals, supporting a possible role of ADCC in vaccine-mediated metastatic inhibition.

The increased T cell infiltration in metastatic lungs, even though not statistically significant, is also promising and can be justified by the antibody-mediated inhibition of xCT function. Indeed, it has been shown that xCT inhibition results in a decrease of β-catenin transcriptional activity,[7] which inversely correlates with CD8$^+$ T cell infiltration[45] while it is associated with infiltration of T regulatory cells and their survival.[46]

AX09-0M6 is initially being developed as an adjuvant therapy for TNBC, due to the high frequency of xCT expressing BCSC found in these tumors, the high rates of relapse and metastatic progression and the lack of targeted therapies. However, research suggests that AX09-0M6 may be of benefit to patients with other indications. The xCT protein is expressed in BCSC and differentiated breast cancer cells in a subset of patients presenting with a variety of breast cancer subtypes, suggesting that xCT positive patients who become refractive to frontline, targeted breast cancer therapy may benefit from AX09-0M6 treatment. Among the others, pancreatic,[24] gastrointestinal,[23] glioblastoma[47] and colorectal[20]
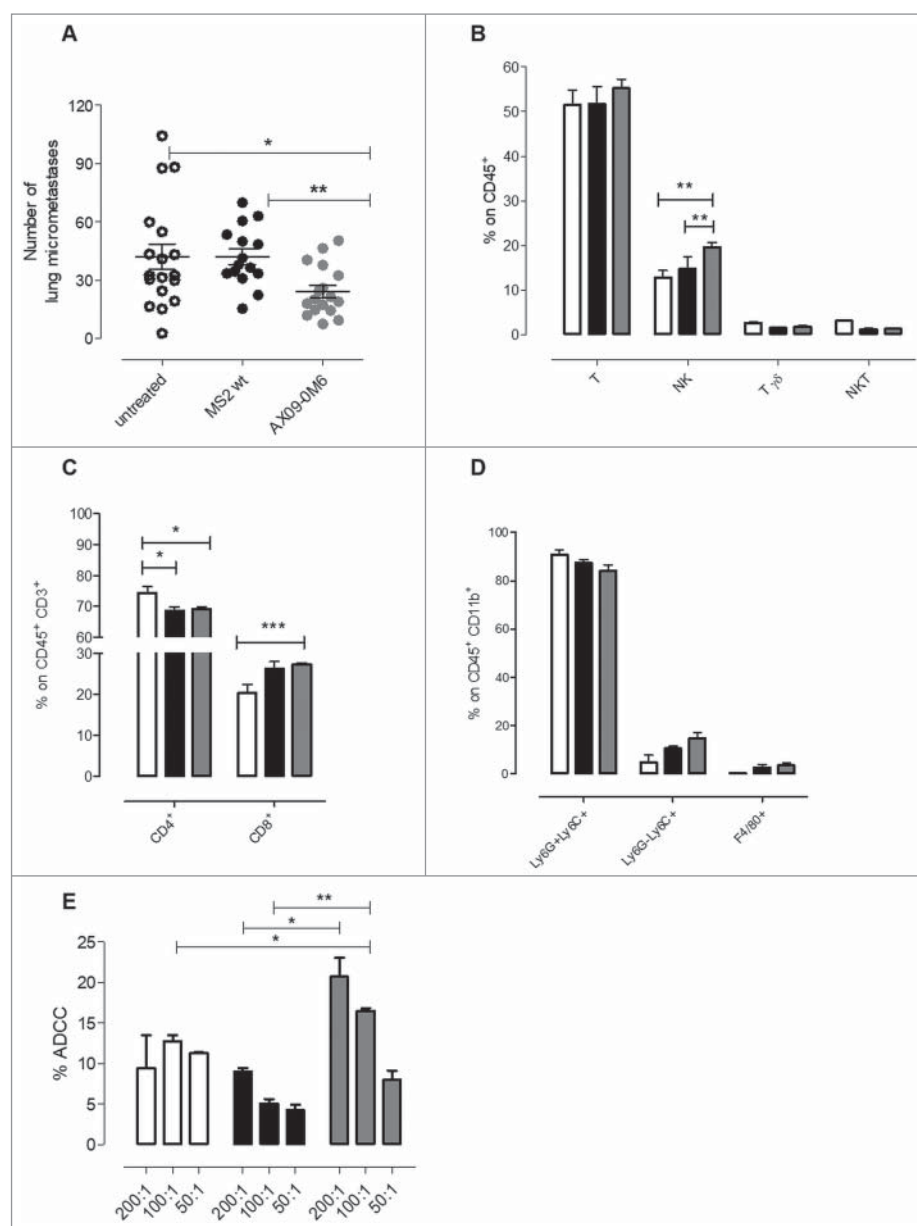
Figure 6. AX09-0M6 attenuates metastases *in vivo* affecting the immune infiltrate and induces antibodies stimulating ADCC. (A) Mice were treated with MS2 wt or AX09-0M6 in the absence of exogenous adjuvant. One week after final administration, P2 tumorspheres derived from TUBO cells were injected into the tail vein of treated mice. 20 days after cell challenge, the lungs were removed, sectioned and the number of micrometastases was determined. Each dot represents a single animal and is the average number of lung metastases from at least 2 sections. Results shown are the aggregate from 3 independent experiments. *, P = 0.0293; **, P = 0.0025, Mann Whitney test. (B-D) Cytofluorimetric analysis of immune infiltrates in lungs of mice left untreated (white bars) or vaccinated with MS2 wt (black bars) or AX09-0M6 (gray bars). (B) Graph shows the percentage ± SEM of CD45$^+$ cells expressing the markers of T (CD3$^+$CD49b$^-$), NK (CD3$^-$CD49b$^+$), $\gamma\delta$ T (CD3$^+\gamma\delta^+$), and NKT (CD3$^+$CD49b$^+$) cells. (C) Percentage ± SEM of CD4$^+$ or CD8$^+$ cells among the CD45$^+$CD3$^+$ T cell population. (D) Percentage ± SEM of Ly6G$^+$Ly6C$^+$ neutrophils, Ly6G$^-$Ly6C$^+$ monocytic MDSC and F4/80$^+$ macrophages among the CD45$^+$CD11b$^+$ myeloid cell population. Three independent experiments were performed and a representative one is shown. E) ADCC assay was performed using 4T1 target cells incubated with 1:50 pooled sera from vaccinated mice (AX09-0M6, gray bars; MS2 wt, black bars and untreated, white bars) and SPC effector cells at different effector/target cells ratios (200:1, 100:1, and 50:1). Results shown are the mean ± SEM of the percentage of ADCC. *, P < 0.05; **, P < 0.01, ***, P < 0.001, Student's *t*-test.

CSC express xCT and inhibition of xCT functions in preclinical models of these cancers using SASP showed reduced metastases and tumor growth.

AX09-0M6 has potential as an add-on therapy for conventional and emerging frontline therapies. Many chemotherapeutic agents upregulate xCT protein in more differentiated cancer cells, which conveys resistance to many of these therapies.[12,15,48,49] Therefore, AX09-0M6 inhibition of xCT function in combination, or sequentially, with chemotherapy may elicit

clinical benefit by sensitizing bulk tumors to chemotherapeutic agents as well as targeting BCSC. The use of blocking monoclonal antibodies to the checkpoint inhibitor Programmed Death-Ligand 1 molecule (PD-L1) is currently in trials for TNBC.[50] PD-L1 is expressed on human CSC and a preliminary FACS experiment shows that PD-L1 is also expressed on 4T1-derived BCSC (data not shown). The combination of AX09-0M6 therapy with PD-L1 blockade may be more effective in reducing BCSC function while still blocking the PD1-PD-L1 axis in the
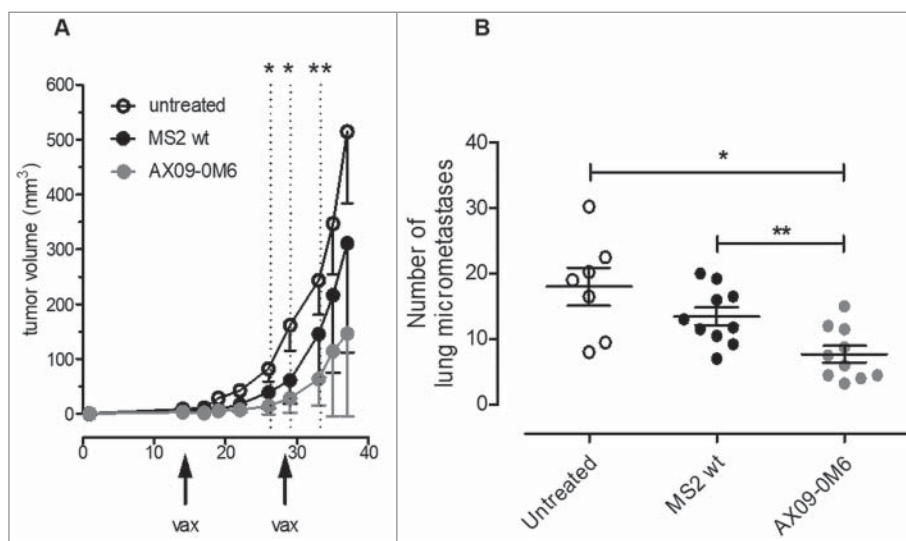
Figure 7. AX09-0M6 is efficacious in preventative and therapeutic models of aggressive breast cancer. (A) Passage 1 tumorspheres derived from 4T1 cells were injected into the inguinal mammary fat pad. When the tumors reached 1 – 1.5 mm in diameter, mice were treated with MS2 wt and AX09-0M6, and boosted 14-days later. Primary tumor diameters were measured at the indicated time-points and tumor volume was calculated. Results shown are the average tumor volume from two independent experiments and the error bars represent the standard deviation of the mean. AX09-0M6 vs MS2 wt: *, $P < 0.05$; **, $P < 0.005$; Student's t test. AX09-0M6 vs untreated: $P < 0.005$ from week 26 to 33; $P < 0.05$ from week 35; Student's t-test. (B) Mice from A were euthanized 40 days after tumor challenge and the number of micrometasta-ses was enumerated. Each dot represents a single animal and is the average number of lung metastases from at least 2 sections. *, $P = 0.0126$; **, $P = 0.0046$, Mann Whit-ney test. Results shown are the aggregate from 2 independent experiments.

tumor bulk. Studies investigating combination therapies with AX09-0M6 are being planned.

Targeting self-antigens can raise safety concerns about effecting normal cells and the induction of autoimmune disease. The xCT protein is highly restricted to a few normal cell types, mostly myeloid cells in the spleen and astrocytes and microglia in the central nervous system. We have observed no toxicity when inhibiting xCT function *in vivo* using AX09-0M6 and DNA-based vaccines. In particular, no inflammatory cell infiltrates or any other abnormalities were detected in brains from both BALB/c and CD-1 mice immunized with AX09-0M6. We believe this result is particularly valuable for the clinical development of AX09-0M6 because it shows that the vaccine generates very robust antibody response in both inbred and outbred mice (e.g. representative of human diversity) with apparently limited or no toxicity.

VLPs targeting both self-antigens and infectious agents (including FDA approved VLP-based vaccines) have demonstrated excellent safety profiles in the clinic. While VLPs elicit high titer antibodies against self-antigens, these antibody responses wane over time. Pharmacokinetic data in human clinical trials performed by Cytos using a similar bacteriophage VLP as AX09-0M6, showed antibody titers against self-antigens had half-lives of ~3 months, which is in stark contrast to long-lived antibody responses using VLP-based vaccines targeting pathogens.[51–53] There has been no evidence for antibody boosting by tissue expression of the endogenous self-antigen in animal models, presumably because foreign T-cell helper responses are required to boost antibody production. Therefore, the duration and magnitude of xCT antibodies are controlled by AX09-0M6 dose and dosing schedule, reducing the possibility of autoimmune disease. Also, the xCT octamer (amino acids 443–450) carried by AX09-0M6 is smaller than effective T-cell epitopes, which nearly

eliminates the potential of inducing an autoreactive xCT T-cell response. This apparent lack of a CTL response against xCT was endorsed by the inability of SPC from AX09-0M6 vaccinated mice to kill 4T1 cells *in vitro* and to upregulate CD107a/b expression after 6 days of co-culture with xCT$^+$ 4T1 cells (data not shown). Nevertheless, the vaccine clearly elicits a T helper 1 response, as indicated by the production of IgG2a against xCT, but this T cell response is against T cell epitopes provided by the VLP proteins that act as carriers.[52,54,55] The small size of the xCT epitope carried by AX09-0M6, however, also increases the probability of homology to other proteins and possible off target affects. Indeed, xCT is one member of a large, highly homologous family of heterogeneous amino acid transporters,[56] most of which are widely expressed by normal tissues and/or have been reported to be upregulated in a variety of tumors.[57] We have blasted the ECD6 peptide with the sequence of most members of the Hetero-meric Aminoacid Transporters family, including LAT1,[58] the most highly homologous to xCT, showing that it is not shared. Further protein homology and cellular localization bioinformatics will be used to identify any other potential cross-reactive target.

Ultimately, a VLP-based immunotherapy with no toxicity has a great potential to be used in a maintenance/neo-adjuvant setting for TNBC before tumor recurrence/refractory. AX09-0M6 could slow or stop the cancer's return by blocking residual CSC that represents a major barrier towards effective cancer treatments.

Materials and methods

Cell and tumorsphere generation

4T1 and HCC-1806 cells were grown in RPMI-1640 Medium (Invitrogen, Corp.) supplemented with 10% heat-inactivated Fetal Bovine Serum (FBS; Sigma-Aldrich). MDA-MB-231 cells

were grown in Dulbecco's Modified Eagle Medium (DMEM, Invitrogen Corp.) supplemented with 10% FBS. All cells were purchased from ATCC (LGC Standards). TUBO cells[59] were cultured in DMEM supplemented with 20% FBS. Each culture medium was supplemented with Penicillin (100 U/mL) and Streptomycin (100 U/mL) (Sigma-Aldrich). Cells were cultured at 37°C in a 5% CO_2 incubator and all cells were tested negative for mycoplasma using polymerase chain reaction (PCR) MycoAlert assay (Lonza). Passage 1 and passage 2 (P1 and P2) tumorspheres were generated as previously described.[39]

Production and purification of VLPs

Production and purification of single-chain dimer versions of MS2 bacteriophage VLPs were done as described.[60] Briefly, ECD6 peptide sequence (LYSDPFST) derived from the sixth loop of xCT protein was inserted genetically into the AB loop of MS2 CP through pDSP62 plasmid as previously described.[32] Plasmids were electroporated into the *E. coli*, T7 expression strain C41 (DE3) (Lucigen), grown to mid-log phase and VLP expression was induced by the addition of IPTG (1 mM, Sigma-Aldrich) overnight at ∼ 30°C. Bacteria pellets were lysed in lysis buffer (50 mM Tris-HCl, pH 8.5, 100 mM NaCl, 10 mM EDTA), sonicated and purified from bacterial debris by centrifugation. Bacterial DNA was removed by treating the supernatant with DNaseI (10 units/mL, 1 hour at 37°C; Sigma-Aldrich) and the VLPs were purified by size exclusion chromatography (Sepharose CL-4B resin, Sigma-Aldrich). Buffer exchange (Phosphate-buffered saline, PBS) and concentration of purified VLPs was achieved using ultrafiltration (Amicon Ultrafiltration device, 100Kd MWCO) and resulting VLP preparations were quantitated by Bradford assay (BioRad). VLP purity was assessed by agarose and SDS-PAGE gel electrophoresis.

Purification of IgG for in vitro assays

Female BALB/c mice were administered 10 μg of VLP without exogenous adjuvant by intramuscular (i.m.) injection followed by a single boost 28 days later. Two weeks after final boost, blood was collected by cardiocentesis and immune sera were isolated as previously described.[61] Total IgG were purified from sera using affinity chromatography (Protein A/G Plus Agarose, Pierce) following manufacturer's protocol. Eluted fractions containing IgG as assessed by SDS-PAGE analysis were concentrated into PBS using ultrafiltration (Amicon Ultrafiltration device, 10 Kd MWCO) and protein concentration was determined by Bradford assay using a mouse IgG standard curve (BioRad). Purified IgG was aliquoted and stored at −20°C.

Characterization of antibody responses

xCT specific antibody responses were evaluated by ELISA using ECD6 peptide (synthesized with a CGG linker at the C-terminus; GenScript) as coating antigen. Avidin (Pierce) prepared in PBS pH 7.5 was added to wells of Immulon 2HB ELISA Plates (Thermo Scientific) at 500 ng/well and incubated for 2 h at 37°C. Following washing, SMPH (Succinimidyl 6-((beta-maleimidopropionamido)hexanoate); Thermo Scientific) was added

to wells at 1 μg/well and incubated for 2 h at 37°C. ECD6 peptide was added at 1 μg/well and incubated overnight at 4°C. Plates were blocked with 0.5% milk in PBS at room temperature for 1 h, and 3-fold dilutions (starting at 1:500) of sera from individual animals were added to each well and incubated for 2 h. Wells were probed with HRP-labeled goat anti-mouse IgG (Invitrogen; 1:5000) for 1 h. The reaction was developed with TMB Solution (3′,3′,5′,5′-Tetramethylbenzidine, Calbiochem) for 1 h and the reaction was stopped using 1% HCl. ECD6 reactivity was determined by measuring optical density (OD) at 450 nm. Wells with twice the OD_{450} value of background (sera from MS2 wt mice) were considered positive and the highest dilution with a positive value was considered the endpoint dilution titer.

To determine IgG subclass elicited by VLP administration, ELISA plates were coated as above. Total IgG and each IgG subclass were measured in triplicate from each animal using a sera dilution of 1:500. Wells were probed with HRP-labeled goat anti-mouse IgG, IgG1, IgG2a, and IgG2b (Invitrogen; 1:5000) for 1 h. Detection was as described above. Relative ratio of each IgG subclass was calculated by taking the average OD_{450} value from IgGx divided by the average OD_{450} from total IgG.

Immune sera effect on tumorspheres

P1 tumorspheres were dissociated and cultured at a density of 6×10^4 cells/ml in a 6-well dish in the absence or presence of 50 μg/ml of purified IgG or of 50 μM SASP (sulfasalazine; Sigma-Aldrich). After 5 days P2 tumorspheres were imaged with an ApoTome fluorescence microscope (Zeiss) and sphere diameter measured with the AxioVision 4.8 software as described.[62] Spheres were counted and reported as number of spheres generated for every 10^3 cells plated, then they were dissociated and processed for FACS analysis of Aldefluor and ROS.

Immunofluorescence

P2 tumorspheres were cytospinned to glass slides, fixed in 4% formalin solution and then blocked in 10% bovine serum albumin (BSA, Sigma-Aldrich). Slides were incubated with 100 μg/ml of purified IgG or 1:10 dilution of sera from CD-1 mice for one hour at room temperature, washed with PBS and incubated with rabbit AlexaFluor488-anti-mouse (Life Technologies).[63] Nuclei were stained with DAPI (Sigma-Aldrich). Images were acquired with a Leica TCS-SP5 II confocal microscope and analyzed using LASAF software (Leica). Fluorescence was quantitated using ImageJ and signal was calculated as integrated density normalized to nuclei number.

In vivo treatments

Female 6- to 8-week-old BALB/c mice (Charles River Laboratories Italia) were maintained at the Molecular Biotechnology Center, University of Torino, and treated in accordance with the University Ethical Committee and European guidelines under Directive 2010/63. Vaccination, performed either before (preventive model) or after tumor challenge (therapeutic model), consisted of two i.m. injections at 2 week intervals. Each mouse

received 5-10 μg of MS2 wt or AX09-0M6, formulated in PBS for a total volume of 50 μL. In the preventive model, one week after last vaccination 5×10^4 tumorspheres derived from TUBO cells were injected i.v.. Mice were sacrificed at 20 days after cell challenge.[39] In the therapeutic model, 1×10^4 P1 4T1 tumorsphere-derived cells were injected s.c. and when the tumor reached a mean diameter of 1-1.5 mm, mice were vaccinated as described above. Tumors were then measured twice a week with calipers in two perpendicular diameters. Tumor growth was reported as volume calculated as $(\pi/6) \times A^2 \times B$,[64] where A and B represent the short and long diameters, respectively. Mice were euthanized 40 days after tumor cell challenge. At sacrifice, blood was collected by cardiocentesis and sera were stored at -20°C for use in immunoassays. Lungs were removed, the right lung was fixed in formaldehyde solution (4%), paraffin embedded, sectioned, and Hematoxylin and Eosin (H&E) stained. Micrometastases were counted with a Nikon SMZ1000 stereomicroscope and analyzed using ImageJ software (U.S. National Institutes of Health).

FACS analysis

Tumorsphere derived cells were stained with Aldefluor kit (Stem Cell Technologies) as reported.[39] To measure intracellular ROS content, cells were stained with 2',7'-dihydrochlorofluorescein diacetate (DHCF-DA, Sigma-Aldrich) as described.[12] To quantify anti-xCT antibody titers, 5×10^5 tumorsphere-derived cells were incubated for 30 min at 4°C with 50 μg/mL of IgG purified from sera of vaccinated mice. Cells were pre-treated with Fc receptor (FcR) blocker (CD16/CD32; Becton Dickinson) for 5 min at 4°C. After washes with PBS containing 2% BSA (Sigma-Aldrich) and 0.1% sodium azide (NaN$_3$; Sigma-Aldrich), cells were incubated with a 1:50 dilution of a FITC-conjugated anti-mouse IgG antibody (DakoCytomation) for 30 min at 4°C.[65] Rabbit anti-xCT Ab (Thermo Fisher Scientific) followed by FITC-conjugated anti-rabbit IgG Ab (DakoCytomation) was used as a positive control on cells fixed and permeabilized with BD Cytofix/Cytoperm kit (Becton Dickinson). Washed cells were then acquired on the BD FACSVerse and analyzed with BD FACSuite^{TM} software (Becton Dickinson). The results were expressed as percentage of positive cells and as mean fluorescence intensity (MFI).

For the analysis of immune infiltrates, lungs from vaccinated mice were finely minced with scissors and then digested by incubation with 1 mg/ml collagenase IV (Sigma Aldrich) in RPMI-1640 (Life Technologies) at 37°C for 1 h in an orbital shaker. After washing in PBS supplemented with 2% FBS, the cell suspension was incubated with a buffer for erythrocyte lysis (155 mM NH$_4$Cl, 15.8 mM Na$_2$CO$_3$, 1 mM EDTA, pH 7.3) for 10 minutes at R.T., then passed through a 70-μm pore cell strainer, centrifuged at 1400 rpm for 10 min and re-suspended in PBS, treated with Fc receptor blocker as described.[66] Cells were then stained with the following Abs: anti-mouse CD45 VioGreen, anti-mouse CD3 FITC, anti-mouse CD4 APC-Vio770, anti-mouse CD8 VioBlue, anti-mouse $\gamma\delta$ PE/Vio770, anti-mouse CD49b PE, anti-mouse F4/80 PE/Vio770, anti-mouse CD11b FITC, anti-mouse Ly6G Vioblue, and anti-mouse Ly6C APC/Vio770 (all from Miltenyi Biotec). For the analysis of xCT expression on myeloid SPC, spleens from vaccinated mice were smashed on a 70-μm pore cell strainer,

erythrocytes were lysed, FcR blocker and cells were stained with anti-mouse CD45 VioGreen, anti-mouse F4/80 PE/Vio770, anti-mouse Ly6G Vioblue, anti-mouse Ly6C APC/Vio770, anti-mouse class II HLA APC (Miltenyi Biotec) and anti-mouse CD206 PE (eBioscience). After washing, cells were fixed and permeabilized with BD Cytofix/Cytoperm kit and stained with rabbit anti-xCT Ab followed by FITC-conjugated anti-rabbit IgG Ab. Samples were acquired on a BD FACSVerse and analyzed using the BD FACSuite software.

Antibody-dependent cell-mediated cytotoxicity (ADCC)

1×10^4 4T1 target cells were labeled with 2 μM of carboxyfluorescein diacetate succinimidyl ester (CFSE; Molecular Probes) following the manufacturer's instructions. ADCC was initiated by the addition of SPC from untreated BALB/c mice as effector cells (200:1, 100:1, and 50:1 as the effector: target (E: T) ratio) and sera from vaccinated mice at a 1:50 dilution. The plate was incubated overnight at 37°C, then cells were harvested, stained with 1μg/ml 7-Amino-Actinomycin D (7-AAD, BD Bioscience), acquired on the BD FACSVerse and analyzed by BD FACSuite^{TM} software (Becton Dickinson). Percent killing was obtained by back-gating on the CFSE$^+$ targets and measuring the % of 7-AAD$^+$ dead cells. % ADCC for each serum sample was calculated with the formula [(dead targets in sample (%) – spontaneously dead targets (%))/(dead target maximum-spontaneously dead targets (%))] $\times$ 100. Spontaneous release was obtained by incubating target cells in medium with serum, whereas maximal release was obtained after treatment with triton solution.

Histological and immunohistochemical analysis

Mice were killed by anaesthesia overdose, and explanted brains were fixed in 4% formalin for 24 hours and then sliced in coronal sections and processed for histology.[67] Paraffin sections were cut at 5 μm and stained with Haematoxylin and Eosin (H&E) or with immunohistochemical antibodies. For the immunohistochemical detection of microglial cells, non-specific immunoreactivity was blocked by incubation of the brain sections with 5% goat serum and 3% milk. The slides were incubated for 1 hour with a rat anti-mouse F4/80 primary antibody (Abcam, CI:A3-1). Biotinylated anti-rat secondary antibody (Dako) was used and the avidin-biotin-peroxidase complex (ABC reaction, Vector Lab) was visualized with diaminobenzidine. (Thermo Scientific). Sections were counterstained with haematoxylin before dehydration and mounting. Slides were digitized with the Panoramic Desk scanner and subsequently evaluated by a pathologist with Panoramic Viewer (both from 3D HISTECH).

Statistical analysis

Differences in sphere formation, protein expression, number of infiltrating cells and proliferation index were evaluated by a Student's t-test. Differences in number of metastases were evaluated by a non-parametric Mann Whitney test. Data are shown as mean $\pm$ SEM unless otherwise stated. Values of $P < 0.05$ were considered significant.

Conflict of interest

Acknowledgments

ORCID

John P. O'Rourke http://orcid.org/0000-0002-7298-1763
Federica Cavallo http://orcid.org/0000-0003-4571-1060

References

1. Bianchini G, Balko JM, Mayer IA, Sanders ME, Gianni L. Triple-negative breast cancer: challenges and opportunities of a heterogeneous disease. Nat Rev Clin Oncol. 2016;13:674–90. doi:10.1038/nrclinonc.2016.66.

2. Visvader JE, Stingl J. Mammary stem cells and the differentiation hierarchy: current status and perspectives. Genes & Dev. 2014;28:1143–58. doi:10.1101/gad.242511.114.

3. Visvader JE, Lindeman GJ. Cancer stem cells in solid tumours: accumulating evidence and unresolved questions. Nat Rev Cancer. 2008;8:755–68. doi:10.1038/nrc2499.

4. Fulawka L, Donizy P, Halon A. Cancer stem cells–the current status of an old concept: literature review and clinical approaches. Biol Res. 2014;47:66. doi:10.1186/0717-6287-47-66. PMID:25723910.

5. Magee JA, Piskounova E, Morrison SJ. Cancer stem cells: impact, heterogeneity, and uncertainty. Cancer Cell. 2012;21:283–96. doi:10.1016/j.ccr.2012.03.003.

6. Nagano O, Okazaki S, Saya H. Redox regulation in stem-like cancer cells by CD44 variant isoforms. Oncogene. 2013;32:5191–8. doi:10.1038/onc.2012.638.

7. Chen RS, Song YM, Zhou ZY, Tong T, Li Y, Fu M, Guo XL, Dong LJ, He X, Qiao HX, et al. Disruption of xCT inhibits cancer cell metastasis via the caveolin-1/beta-catenin pathway. Oncogene. 2009;28:599–609. doi:10.1038/onc.2008.414.

8. Guo W, Zhao Y, Zhang Z, Tan N, Zhao F, Ge C, Liang L, Jia D, Chen T, Yao M, et al. Disruption of xCT inhibits cell growth via the ROS/autophagy pathway in hepatocellular carcinoma. Cancer Lett. 2011;312:55–61. doi:10.1016/j.canlet.2011.07.024. PMID:21906871.

9. Gasol E, Jimenez-Vidal M, Chillaron J, Zorzano A, Palacin M. Membrane topology of system xc- light subunit reveals a re-entrant loop with substrate-restricted accessibility. J Biol Chem. 2004;279:31228–36. doi:10.1074/jbc.M402428200.

10. Sato H, Tamba M, Okuno S, Sato K, Keino-Masu K, Masu M, Bannai S. Distribution of cystine/glutamate exchange transporter, system x (c)-, in the mouse brain. J Neurosci: the official journal of the Society for Neuroscience. 2002;22:8028–33.

11. Miyazaki I, Murakami S, Torigoe N, Kitamura Y, Asanuma M. Neuroprotective effects of levetiracetam target xCT in astrocytes in parkinsonian mice. J Neurochem. 2016;136:194–204. doi:10.1111/jnc.13405.

12. Lanzardo S, Conti L, Rooke R, Ruiu R, Accart N, Bolli E, Arigoni M, Macagno M, Barrera G, Pizzimenti S, et al. Immunotargeting of Antigen xCT Attenuates Stem-like Cell Behavior and Metastatic Progression in Breast Cancer. Cancer Res. 2016;76:62–72. doi:10.1158/0008-5472.CAN-15-1208.

13. Briggs KJ, Koivunen P, Cao S, Backus KM, Olenchock BA, Patel H, Zhang Q, Signoretti S, Gerfen GJ, Richardson AL, et al. Paracrine Induction of HIF by Glutamate in Breast Cancer: EglN1 Senses Cysteine. Cell. 2016;166:126–39. doi:10.1016/j.cell.2016.05.042.

14. Gyorffy B, Lanczky A, Eklund AC, Denkert C, Budczies J, Li Q, Szallasi Z. An online survival analysis tool to rapidly assess the effect of 22,277 genes on breast cancer prognosis using microarray data of 1,809 patients. Breast Cancer Res Treat. 2010;123:725–31. doi:10.1007/s10549-009-0674-9.

15. Lu H, Samanta D, Xiang L, Zhang H, Hu H, Chen I, Bullen JW, Semenza GL. Chemotherapy triggers HIF-1-dependent glutathione synthesis and copper chelation that induces the breast cancer stem cell phenotype. Proc Natl Acad Sci U S A. 2015;112:E4600−9. doi:10.1073/pnas.1513433112.

16. Nishino M, Ozaki M, Hegab AE, Hamamoto J, Kagawa S, Arai D, Yasuda H, Naoki K, Soejima K, Saya H, et al. Variant CD44 expression is enriching for a cell population with cancer stem cell-like characteristics in human lung adenocarcinoma. J Cancer. 2017;8:1774–85. doi:10.7150/jca.19732.

17. Polewski MD, Reveron-Thornton RF, Cherryholmes GA, Marinov GK, Aboody KS. SLC7A11 Overexpression in Glioblastoma Is Associated with Increased Cancer Stem Cell-Like Properties. Stem Cells Dev. 2017. doi:10.1089/scd.2017.0123. PMID:28610554.

18. Song Y, Jang J, Shin TH, Bae SM, Kim JS, Kim KM, Myung SJ, Choi EK, Seo HR. Sulfasalazine attenuates evading anticancer response of CD133-positive hepatocellular carcinoma cells. Journal of experimental & clinical cancer research: CR. 2017;36:38. doi:10.1186/s13046-017-0511-7.

19. Zavros Y. Initiation and Maintenance of Gastric Cancer: A Focus on CD44 Variant Isoforms and Cancer Stem Cells. Cell Mol Gastroenterol Hepatol. 2017;4:55–63. doi:10.1016/j.jcmgh.2017.03.003.

20. Ju HQ, Lu YX, Chen DL, Tian T, Mo HY, Wei XL, Liao JW, Wang F, Zeng ZL, Pelicano H, et al. Redox Regulation of Stem-like Cells Though the CD44v-xCT Axis in Colorectal Cancer: Mechanisms and Therapeutic Implications. Theranostics. 2016;6:1160–75. doi:10.7150/thno.14848.

21. Yoshikawa M, Tsuchihashi K, Ishimoto T, Yae T, Motohara T, Sugihara E, Onishi N, Masuko T, Yoshizawa K, Kawashiri S, et al. xCT inhibition depletes CD44v-expressing tumor cells that are resistant to EGFR-targeted therapy in head and neck squamous cell carcinoma. Cancer Res. 2013;73:1855–66. doi:10.1158/0008-5472.CAN-12-3609-T.

22. Hasegawa M, Takahashi H, Rajabi H, Alam M, Suzuki Y, Yin L, Tagde A, Maeda T, Hiraki M, Sukhatme VP, et al. Functional interactions of the cystine/glutamate antiporter, CD44v and MUC1-C oncoprotein in triple-negative breast cancer cells. Oncotarget. 2016;7:11756–69. doi:10.18632/oncotarget.7598.

23. Ishimoto T, Nagano O, Yae T, Tamada M, Motohara T, Oshima H, Ikeda T, Asaba R, Yagi H, Masuko T, et al. CD44 variant regulates redox status in cancer cells by stabilizing the xCT subunit of system xc (-) and thereby promotes tumor growth. Cancer cell. 2011;19:387–400. doi:10.1016/j.ccr.2011.01.038.

24. Pore N, Jalla S, Liu Z, Higgs B, Sorio C, Scarpa A, Hollingsworth R, Tice DA, Michelotti E. In Vivo Loss of Function Screening Reveals Carbonic Anhydrase IX as a Key Modulator of Tumor Initiating Potential in Primary Pancreatic Tumors. Neoplasia. 2015;17:473–80. doi:10.1016/j.neo.2015.05.001.

25. Guan J, Lo M, Dockery P, Mahon S, Karp CM, Buckley AR, Lam S, Gout PW, Wang YZ. The xc- cystine/glutamate antiporter as a potential therapeutic target for small-cell lung cancer: use of sulfasalazine. Cancer Chem Pharmacol. 2009;64:463–72. doi:10.1007/s00280-008-0894-4.

26. Timmerman LA, Holton T, Yuneva M, Louie RJ, Padro M, Daemen A, Hu M, Chan DA, Ethier SP, van 't Veer LJ, et al. Glutamine sensitivity analysis identifies the xCT antiporter as a common triple-negative breast tumor therapeutic target. Cancer cell. 2013;24:450–65. doi:10.1016/j.ccr.2013.08.020.

27. Robe PA, Martin DH, Nguyen-Khac MT, Artesi M, Deprez M, Albert A, Vanbelle S, Califice S, Bredel M, Bours V. Early termination of ISRCTN45828668, a phase 1/2 prospective, randomized study of sulfasalazine for the treatment of progressing malignant gliomas in adults. BMC Cancer. 2009;9:372. doi:10.1186/1471-2407-9-372. PMID:19840379.

28. Gout PW, Buckley AR, Simms CR, Bruchovsky N. Sulfasalazine, a potent suppressor of lymphoma growth by inhibition of the x(c)- cystine transporter: a new action for an old drug. Leukemia. 2001;15:1633–40.

29. Andreasson K, Tegerstedt K, Eriksson M, Curcio C, Cavallo F, Forni G, Dalianis T, Ramqvist T. Murine pneumotropic virus chimeric Her2/neu virus-like particles as prophylactic and therapeutic vaccines against Her2/neu expressing tumors. International journal of cancer Journal international du cancer. 2009;124:150–6. doi:10.1002/ijc.23920.

30. Bachmann MF, Jennings GT. Vaccine delivery: a matter of size, geometry, kinetics and molecular patterns. Nat Rev Immunol. 2010;10:787–96. doi:10.1038/nri2868.

31. Tumban E, Muttil P, Escobar CA, Peabody J, Wafula D, Peabody DS, Chackerian B. Preclinical refinements of a broadly protective VLP-based HPV vaccine targeting the minor capsid protein, L2. Vaccine. 2015;33:3346–53. doi:10.1016/j.vaccine.2015.05.016.

32. Chackerian B, Caldeira Jdo C, Peabody J, Peabody DS. Peptide epitope identification by affinity selection on bacteriophage MS2 virus-like particles. Journal of molecular biology. 2011;409:225–37. doi:10.1016/j.jmb.2011.03.072.

33. Caldeira Jdo C, Medford A, Kines RC, Lino CA, Schiller JT, Chackerian B, Peabody DS. Immunogenic display of diverse peptides, including a broadly cross-type neutralizing human papillomavirus L2 epitope, on virus-like particles of the RNA bacteriophage PP7. Vaccine. 2010;28:4384–93.

34. Peabody DS, Manifold-Wheeler B, Medford A, Jordan SK, do Carmo Caldeira J, Chackerian B. Immunogenic display of diverse peptides on virus-like particles of RNA phage MS2. J mol biol. 2008;380:252–63. doi:10.1016/j.jmb.2008.04.049.

35. Caldeira J, Bustos J, Peabody J, Chackerian B, Peabody DS. Epitope-Specific Anti-hCG Vaccines on a Virus Like Particle Platform. PloS One. 2015;10:e0141407. doi:10.1371/journal.pone.0141407. PMID:26516771.

36. Crossey E, Amar MJ, Sampson M, Peabody J, Schiller JT, Chackerian B, Remaley AT. A cholesterol-lowering VLP vaccine that targets PCSK9. Vaccine. 2015;33:5747–55. doi:10.1016/j.vaccine.2015.09.044.

37. O'Rourke JP, Daly SM, Triplett KD, Peabody D, Chackerian B, Hall PR. Development of a mimotope vaccine targeting the Staphylococcus aureus quorum sensing pathway. PloS one. 2014;9:e111198. doi:10.1371/journal.pone.0111198. PMID:25379726.

38. Lewerenz J, Hewett SJ, Huang Y, Lambros M, Gout PW, Kalivas PW, Massie A, Smolders I, Methner A, Pergande M, et al. The cystine/glutamate antiporter system x(c)(-) in health and disease: from molecular mechanisms to novel therapeutic opportunities. Antioxidants & redox signaling. 2013;18:522–55. doi:10.1089/ars.2011.4391.

39. Conti L, Lanzardo S, Arigoni M, Antonazzo R, Radaelli E, Cantarella D, Calogero RA, Cavallo F. The noninflammatory role of high mobility group box 1/Toll-like receptor 2 axis in the self-renewal of mammary cancer stem cells. FASEB journal: official publication of the Federation of American Societies for Experimental Biology. 2013;27:4731–44. doi:10.1096/fj.13-230201.

40. Pulaski BA, Ostrand-Rosenberg S. Mouse 4T1 breast tumor model. Current protocols in immunology / edited by John E Coligan [et al]. 2001;Chapter 20:Unit 20 2.

41. Tallerico R, Todaro M, Di Franco S, Maccalli C, Garofalo C, Sottile R, Palmieri C, Tirinato L, Pangigadde PN, La Rocca R, et al. Human NK cells selective targeting of colon cancer-initiating cells: a role for natural cytotoxicity receptors and MHC class I molecules. J Immunol. 2013;190:2381–90. doi:10.4049/jimmunol.1201542.

42. Tallerico R, Conti L, Lanzardo S, Sottile R, Garofalo C, Wagner AK, Johansson MH, Cristiani CM, Kärre K, Carbone E, et al. NK cells control breast cancer and related cancer stem cell hematological spread. Oncoimmunology. 2017;6:e1284718. doi:10.1080/2162402X.2017.1284718. PMID:28405511.

43. Lollini PL, Cavallo F, Nanni P, Forni G. Vaccines for tumour prevention. Nat Rev Cancer. 2006;6:204–16. doi:10.1038/nrc1815. PMID:16498443.

44. Cavallo F, Calogero RA, Forni G. Are oncoantigens suitable targets for anti-tumour therapy? Nat Rev Cancer. 2007;7:707–13. doi:10.1038/nrc2208.

45. Spranger S, Bao R, Gajewski TF. Melanoma-intrinsic beta-catenin signalling prevents anti-tumour immunity. Nature. 2015;523:231–5. doi:10.1038/nature14404.

46. Hong Y, Manoharan I, Suryawanshi A, Majumdar T, Angus-Hill ML, Koni PA, Manicassamy B, Mellor AL, Munn DH, Manicassamy S. beta-catenin promotes regulatory T-cell responses in tumors by inducing vitamin A metabolism in dendritic cells. Cancer Res. 2015;75:656–65. doi:10.1158/0008-5472.CAN-14-2377.

47. Sehm T, Fan Z, Ghoochani A, Rauh M, Engelhorn T, Minakaki G, Dörfler A, Klucken J, Buchfelder M, Eyüpoglu IY, et al. Sulfasalazine impacts on ferroptotic cell death and alleviates the tumor microenvironment and glioma-induced brain edema. Oncotarget. 2016;7:36021–33. doi:10.18632/oncotarget.8651.

48. Wang F, Yang Y. Suppression of the xCT-CD44v antiporter system sensitizes triple-negative breast cancer cells to doxorubicin. Breast cancer research and treatment. 2014;147:203–10. doi:10.1007/s10549-014-3068-6.

49. Ma MZ, Chen G, Wang P, Lu WH, Zhu CF, Song M, Yang J, Wen S, Xu RH, Hu Y, et al. Xc- inhibitor sulfasalazine sensitizes colorectal cancer to cisplatin by a GSH-dependent mechanism. Cancer lett. 2015;368:88–96. doi:10.1016/j.canlet.2015.07.031.

50. Emens LA. Breast Cancer Immunotherapy: Facts and Hopes. Clinical cancer research: an official journal of the American Association for Cancer Research 2017; pii: clincanres.3001.2017. doi:10.1158/1078-0432.CCR-16-3001.

51. Tissot AC, Maurer P, Nussberger J, Sabat R, Pfister T, Ignatenko S, Volk HD, Stocker H, Müller P, Jennings GT, et al. Effect of immunisation against angiotensin II with CYT006-AngQb on ambulatory blood pressure: a double-blind, randomised, placebo-controlled phase IIa study. Lancet. 2008;371:821–7. doi:10.1016/S0140-6736(08)60381-5.

52. Ambuhl PM, Tissot AC, Fulurija A, Maurer P, Nussberger J, Sabat R, Nief V, Schellekens C, Sladko K, Roubicek K, et al. A vaccine for hypertension based on virus-like particles: preclinical efficacy and phase I safety and immunogenicity. J Hypertens. 2007;25:63–72. doi:10.1097/HJH.0b013e32800ff5d6.

53. Maurer P, Jennings GT, Willers J, Rohner F, Lindman Y, Roubicek K, Renner WA, Müller P, Bachmann MF. A therapeutic vaccine for nicotine dependence: preclinical efficacy, and Phase I safety and immunogenicity. Eur J Immunol. 2005;35:2031–40. doi:10.1002/eji.200526285.

54. Chackerian B, Rangel M, Hunter Z, Peabody DS. Virus and virus-like particle-based immunogens for Alzheimer's disease induce antibody responses against amyloid-beta without concomitant T cell responses. Vaccine. 2006;24:6321–31. doi:10.1016/j.vaccine.2006.05.059.

55. Spohn G, Schori C, Keller I, Sladko K, Sina C, Guler R, Schwarz K, Johansen P, Jennings GT, Bachmann MF. Preclinical efficacy and safety of an anti-IL-1beta vaccine for the treatment of type 2 diabetes. Mol Ther Methods Clin Dev. 2014;1:14048. doi:10.1038/mtm.2014.48. PMID:26015986

56. Fotiadis D, Kanai Y, Palacin M. The SLC3 and SLC7 families of amino acid transporters. Mol Aspects Med. 2013;34:139–58. doi:10.1016/j.mam.2012.10.007.

57. Bhutia YD, Babu E, Ramachandran S, Ganapathy V. Amino Acid transporters in cancer and their relevance to "glutamine addiction": novel targets for the design of a new class of anticancer drugs. Cancer research. 2015;75:1782–8. doi:10.1158/0008-5472.CAN-14-3745.

58. Geier EG, Schlessinger A, Fan H, Gable JE, Irwin JJ, Sali A, Giacomini KM.. Structure-based ligand discovery for the Large-neutral Amino Acid Transporter 1, LAT-1. Proc Natl Acad Sci U S A. 2013;110:5480–5. doi:10.1073/pnas.1218165110.

59. Conti L, Ruiu R, Barutello G, Macagno M, Bandini S, Cavallo F, Lanzardo S. Microenvironment, oncoantigens, and antitumor vaccination: lessons learned from BALB-neuT mice. BioMed Research International. 2014;2014:534969. doi:10.1155/2014/534969. PMID:25136593.

60. O'Rourke JP, Peabody DS, Chackerian B. Affinity selection of epitope-based vaccines using a bacteriophage virus-like particle platform. Curr Opin Virol. 2015;11:76–82.

61. Porzia A, Lanzardo S, Citti A, Cavallo F, Forni G, Santoni A, Galandrini R, Paolini R.. Attenuation of PI3K/Akt-mediated tumorigenic signals through PTEN activation by DNA vaccine-induced anti-ErbB2 antibodies. J Immunol. 2010;184:4170–7. doi:10.4049/jimmunol.0903375.

62. Conti L, Lanzardo S, Ruiu R, Cadenazzi M, Cavallo F, Aime S, Geninatti Crich S. L-Ferritin targets breast cancer stem cells and delivers therapeutic and imaging agents. Oncotarget. 2016;7:66713–27. doi:10.18632/oncotarget.10920.

63. Riccardo F, Iussich S, Maniscalco L, Lorda Mayayo S, La Rosa G, Arigoni M, De Maria R, Gattino F, Lanzardo S, Lardone E, et al. CSPG4-specific immunity and survival prolongation in dogs with oral malignant melanoma immunized with human CSPG4 DNA. Clinical cancer research: an official journal of the American Association for Cancer Research. 2014;20:3753–62. doi:10.1158/1078-0432.CCR-13-3042.

64. Tomayko MM, Reynolds CP. Determination of subcutaneous tumor size in athymic (nude) mice. Cancer chemotherapy and pharmacology. 1989;24:148–54. doi:10.1007/BF00300234.

65. Regis G, Icardi L, Conti L, Chiarle R, Piva R, Giovarelli M, et al. IL-6, but not IFN-gamma, triggers apoptosis and inhibits in vivo growth of human malignant T cells on STAT3 silencing. Leukemia. 2009;23:2102–8.

66. Macagno M, Bandini S, Stramucci L, Quaglino E, Conti L, Balmas E, Smyth MJ, Lollini PL, Musiani P, Forni G, et al. Multiple roles of perforin in hampering ERBB-2 (Her-2/neu) carcinogenesis in transgenic male mice. J Immunol. 2014;192:5434–41. doi:10.4049/jimmunol.1301248.

67. Jordan WH, Young JK, Hyten MJ, Hall DG. Preparation and analysis of the central nervous system. Toxicologic pathology. 2011;39:58–65. doi:10.1177/0192623310391480.